

## STRENGTHENING OF A REINFORCED CONCRETE BRIDGE WITH PRESTRESSED STEEL WIRE ROPES

*Kexin Zhang, Quansheng Sun*

*Department of Civil Engineering, Northeast Forestry University, Harbin, 150040, China; [zkx0204@yahoo.com](mailto:zkx0204@yahoo.com), [hrbsqs@126.com](mailto:hrbsqs@126.com)*

### ABSTRACT

This paper describes prestressed steel wire ropes as a way to strengthen a 20-year-old RC T-beam bridge. High strength, low relaxation steel wire ropes with minor radius, high tensile strain and good corrosion resistance were used in this reinforcement. The construction process for strengthening with prestressed steel wire ropes—including wire rope measuring, extruding anchor heads making, anchorage installing, tensioning steel wire ropes and pouring mortar was described. Ultimate bearing capacity of the bridge after strengthening was discussed based on the concrete structure theory. The flexural strength of RC T-beam bridges strengthened with prestressed steel wire ropes was governed by the failure of concrete crushing. To investigate effectiveness of the strengthening method, fielding-load tests were carried out before and after strengthening. The results of concrete strain and deflection show that the flexural strength and stiffness of the strengthened beam are improved. The crack width measurement also indicates that this technique could increase the durability of the bridge. Thus, this strengthened way with prestressed steel wire rope is feasible and effective.

### KEYWORDS

Steel Wire Ropes, Prestressed, Strengthening, RC Bridges, Field Application, Load Test

### INTRODUCTION

Transportation agencies are faced with a continuous challenge to keep bridges in a good operating condition. Bridge structures are deteriorating at a fast rate, and costs for maintenance and rehabilitation are continuously rising. It is both economically and environmentally satisfactory to upgrade bridge structures rather than rebuild them if simple, effective, and rapid method can be used.

To improve the working ability of concrete bridges, many techniques have been used in strengthening. The most common methods for strengthening beams are external bonding steel plate, external bounding carbon fibre reinforced polymer (CFRP), and external posttensioning tensions. Despite the capacities, stiffness and cracking performance of the steel plate strengthening beams are improved. Bonding steel plates also show some disadvantages, such as weakened bonding caused by steel corrosion, increased dead load weight and difficulties in adapting to the concrete surface profile [1-3]. CFRP materials have good structural performance, high strength and light weight. CFRP can be easily installed, as they can be attached to a curved profile [4-6]. However, when CFRP are used as externally bonded reinforcement, the flexural stiffness has very little improvement peeling failure is often occurred without warning than un-strengthened flexural members. And that the cost of CFRP is high. Adding prestressing by external tendons can significantly increase the yield load and the ultimate resistance of the beams, the deflection at the serviceability state is also reduced, the behaviour of composite beams prestressed with external tensions was investigated [7-8]. However, a large jack must be provided

for drawing of the pre-stressing tendons and need a big drawing space during construction.

Recently, a new strengthening technique with distributed prestressed high strength steel wire rope was proposed. Unreinforced masonry walls were strengthened with prestressed wire ropes in the laboratory [9]. The proposed strengthening procedure was highly effective in enhancing the in-plane shear strength and ductility of the unreinforced masonry walls. Then the prestressed steel wire mesh strengthened shear walls was studied, the cracking load, yield load, ultimate load of shear wall specimens were increased [10]. Guo [11, 12] investigated the mechanical properties of RC columns strengthened with prestressed steel wire ropes. The stiffness was increased and the stiffness degradation mitigated. The seismic strengthening effect of the reinforced columns with steel wire spacing of 30 mm did not change significantly with increasing of prestressing force level.

In order to study the effect of strengthening concrete beams. Seven RC beams were strengthened with prestressed steel wire ropes by Gang [13, 14]. The effective utilization rate of prestressed steel wire rope strengthening was higher than that of the pasting steel plate and CFRP strengthening. Zhang [15] took the stress loss and the number of steel wire ropes into consideration, and the failure mode as well as improvements of cracking resistance, bending bearing capacity and stiffness were investigated. This strengthening technique for RC beams, which was proposed to overcome the shortcomings of existing strengthening methods, utilises the advantages of traditional materials and achieves an active strengthening of RC beams with less influence on the original structure and better comprehensive performance [13-15]. The advantages of this technique also include minimum site disruption, minimal increase in the size of the repaired member, minimum scaffolding, superiority for fire and corrosion resistance, and low cost.

Nevertheless, these research projects were carried out with laboratory-scale tests and corresponding analyses. Applying and obtaining the application results in engineering are essential. This study describes a novel strengthening method using prestressed steel wire ropes to strengthen a 20-year-old reinforced concrete T-beam bridge in service, including design, field application, field test and analysis.

## BACKGROUND

The bridge discussed in this paper carries Jianbian Farm in Heilongjiang Province, China. This simple span, reinforced concrete, T-beam structure was built in 1995. The bridge is 16.0-m long and about 8.5-m wide, and is supported by a total of 5 beams spaced at 1.6-m centre to centre. A lateral view and a cross-section of the bridge are shown in Figure 1 and Figure 2, respectively. The bridge has been opened to traffic without weight-limit restrictions and carries an average daily traffic of 1200 vehicles. It has two lanes and carries one lane of traffic in each direction.

The bridge has different degrees of damage caused by aging, overload, surging traffic and environment. During routine inspection, salt infiltration and excessive moisture were observed in the bridge superstructure. Many beams had been covered largely with efflorescent concrete. Serious cracks occurred in the edge-beam, as water from the pavement cracks affected the durability of the girder. The diseases of the bridge were seen in Figure 3. Heilongjiang Province Department of Transportation elected to rehabilitate the structure as opposed to replacement or load posting. A prestressed steel wire ropes strengthening method was selected based on its application being the minimum site disruption and the most practice. Strengthening work, including wire rope measuring, extruding anchor heads making, anchorage installing, tensioning and installing steel wire ropes and polymer mortar pouring was completed during July – September of 2015.



Fig. 1 - Lateral view of the bridge

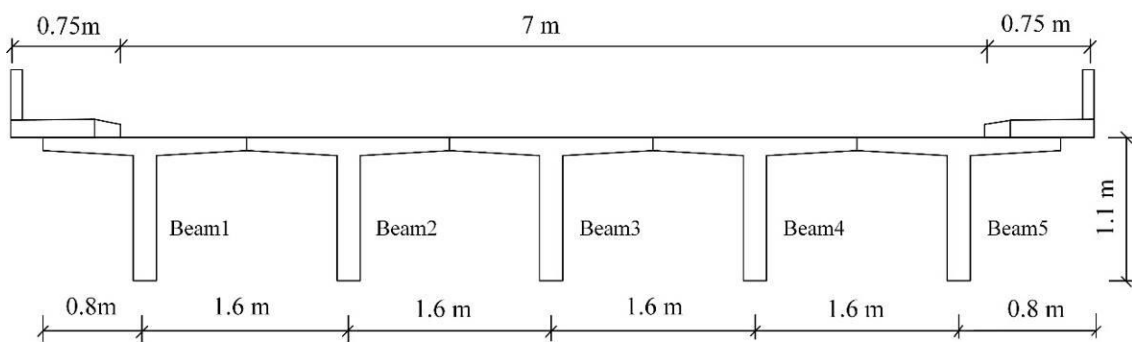


Fig. 2 - Cross-section of the bridge

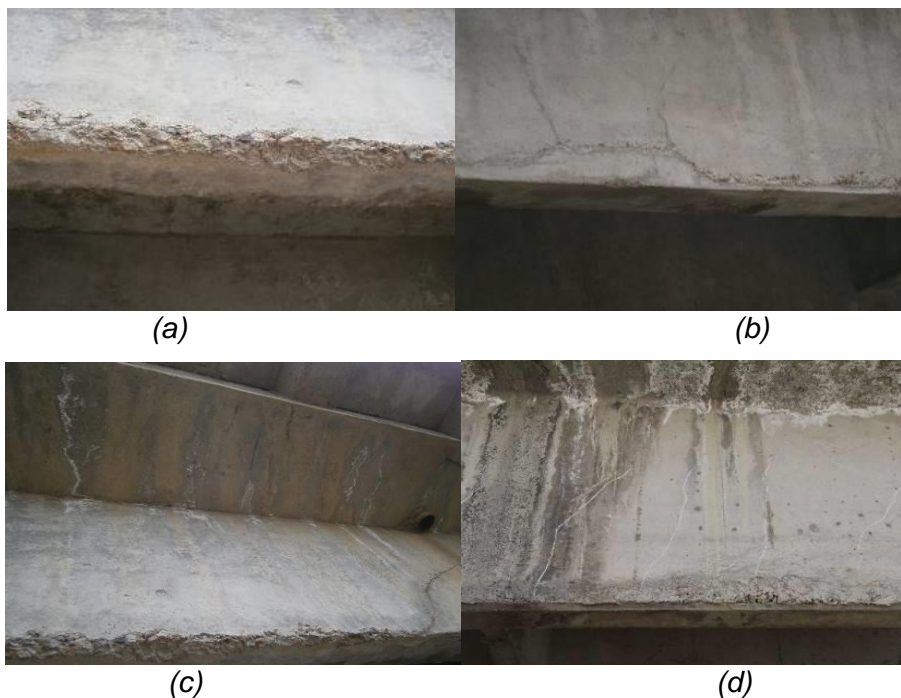


Fig. 3 - Diseases of the bridge; a) efflorescent concrete, b) cracks and efflorescent concrete, c) leakage and efflorescent concrete, d) cracks and leakage

## PRESTRESSED STEEL WIRE ROPES DESIGN AND INSTALLATION

Bridge material properties such as the concrete compression strength and steel yield strength were assumed because the owner of the bridge did not allow coring to obtain the on-site strengths of the materials from the bridge girder. These basic properties  $f_c$   $f_s$  were assumed as described by JTJ023-85 [16] for bridges of that age because no sample could be obtained onsite. Concrete compression strength, concrete elastic modulus, yield strength of steel rebar and elastic modulus of steel rebar are listed in Table 1.

High strength, low relaxation steel wire ropes with minor radius, high tensile strain and good corrosion resistance were used in this reinforcement. High strength steel wire ropes with a normal diameter of 4 mm and normal section of 10.55 mm<sup>2</sup> were chosen. A test was applied to determinate the mechanical properties of the steel wire ropes with lengths of 50 mm as shown in Figure 4. Stress-strain curve is shown in Figure 5. Before the proportional limit point, the curves indicate a fine linear relationship between stress and strain and there is no obvious yield point at the non-linear stage. The ultimate tensile strength was 1250 Mpa and elastic modulus was 130 Mpa. The stress when residual strain was 0.2% is defined to be the normal yield stress, which is about 85% of its ultimate tensile strength. The properties of wire ropes were shown in Table 1.

Tab. 1 - Material properties

Material	Property	Value
Steel wire rope	$f_{ps}$ (MPa)	1250
	$E_{ps}$ (GPa)	130
Concrete	$f_c$ (MPa)	30
	$E_c$ (GPa)	30
Steel	$f_s$ (MPa)	335
	$E_s$ (GPa)	200

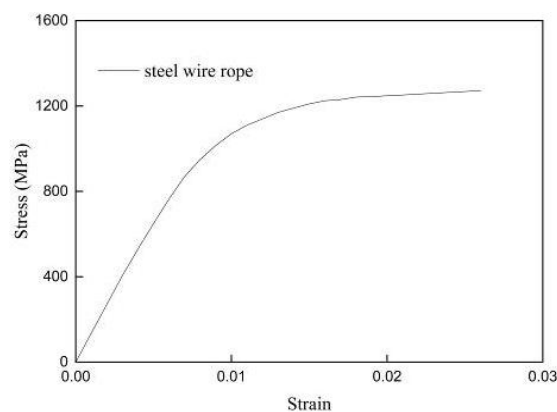


Fig. 4 - Tension test of wire ropes      Fig. 5 - Stress-strain curve of steel wire ropes

### Strengthening analysis

The flexural capacity is established based on force equilibrium, strain compatibility and constitutive laws of materials up to failure. Whitney's rectangular stress block was used to simulate the behaviour of the compressed concrete. Figure 6 shows the strain and stress relationship of beams at the ultimate stage. The bearing strength of the beam equals to 1622.7 kN.m. T-beams strengthened with prestressed wire ropes were the beam flexural failure because of the excellent anchorage performance. The flexural capacity of the reinforced member depended on the concrete

crushing or the steel wire rope rupture. According to strain compatibility, the strain of steel bar  $\epsilon_s$  can be expressed as follows:

$$\epsilon_s = \frac{d_s - x}{d_{ps} - x} \epsilon_{ps} \quad (1)$$

Where  $d_s$  represents the depth from the centroid of steel bars to the top of the T-cross section,  $d_{ps}$  represents the depth from the centroid of the steel wire ropes section to the top of the T-cross section,  $x$  represents the depth of the neutral axis and  $\epsilon_{ps}$  represents the strain of the centroid of the steel wire ropes section.

When steel wire rope failure happens,  $\epsilon_s$  goes beyond the allowance strain of steel rebars, which is 0.01 according to Design Code of Concrete Structures [17]. Therefore, beam failure is not controlled by steel yield.

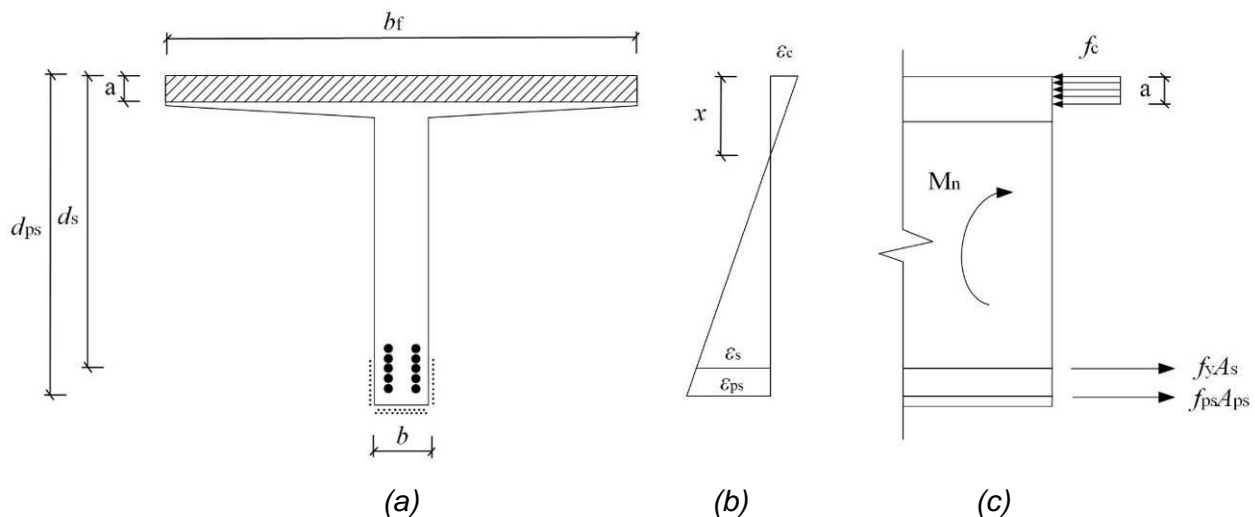


Fig. 6 - Internal strain and stress distribution for a T-shape section ; a ) Reinforced concrete section, b ) Strain distribution, c) Stress distribution

When concrete crushing failure happens, the ultimate compressive strain for the concrete is taken as 0.003.  $\epsilon_s$  is larger than the yield strain of steel rebar and smaller than 0.01 from the relationship of strains between concrete and steel rebar. According to strain compatibility, the strain of the centroid of the steel wire ropes section  $\epsilon_{ps}$  can be expressed as follows.

$$\epsilon_{ps} = \frac{d_{ps} - x}{x} \epsilon_{cu} \quad (2)$$

Due to the steel wire rope is a nearly elastic material, the stress  $\sigma_{ps}$  of the steel wire rope material can be calculated by the following:

$$\sigma_{ps} = E_{ps} \epsilon_{ps} + \sigma_{pe} \quad (3)$$

Where  $\sigma_{pe}$  is the prestress in steel wire ropes, stress relationship of beams at the ultimate stage is seen as Figure 6. From the equilibrium condition:

$$\alpha_1 f_c b_f a = f_y A_s + f_{ps} A_{ps} \quad (4)$$

$$M_u = f_{ps} A_{ps} \left( d_{ps} - \frac{x}{2} \right) + f_y A_s \left( d_s - \frac{x}{2} \right) \quad (5)$$

Where  $M_u$  is the flexural strength of the T-beam strengthened with prestressed steel wire ropes,  $\alpha_1=1$ ,  $a$  is the depth of the equivalent rectangular concrete stress block;  $a=0.8x$ ,  $b_f$  is the width of the flange,  $A_s$  represents the area of the steel bars and  $f_y$  represents the yield stress of the steel bars.

The flexural strength of the beams after strengthening can be calculated through a combination of Equation. (1) - Equation (5).

The above mentioned analysis shows that the bearing capacity of the strengthened beam is controlled by the failure of concrete crushing. The section of the T-beam strengthened by prestressed steel wire ropes is shown in Figure 7. All the steel wire ropes were anchored at one place near the supports. For the double-deck arrangement of wire ropes at the bottom of the beam, the two anchors were arranged separately. The designed tension stress for steel wire ropes is 650MPa. Flexural strength increased to 1075.2 kN.m through prestressed steel wire ropes.

The verification of serviceability limit state was carried out according to Design Code of Concrete Structures [17]. The deflection calculation was as follows:

$$f = \frac{5}{48} \cdot \frac{M_s l^2}{B} \quad (6)$$

Where  $M_s$  is the calculated bending moment for a combination of short-term effects of load;  $l=15.7\text{m}$ ,  $B$  is the flexural rigidity of the equivalent section of the cracking member. The calculated deflection at serviceability limit state after being strengthened with prestressed steel wire ropes was 6.9mm. The value of 6.9mm was less than the value of  $l/600$ , which met the requirement.

The crack width calculation was as follows:

$$w_{\max} = \alpha_{cr} \psi \frac{\sigma_s}{E_s} l_{cr} \quad (7)$$

Where  $M_{cr}$  is the calculated maximum crack width for a standard combination of load effects (considering the long-term effects);  $\alpha_{cr}=1.5$ ;  $\psi=1$ ;  $\sigma_s$  is the equivalent stress of longitudinal tensile reinforcement;  $E_s$  is the elastic modulus of reinforcement,  $l_{cr}=0.2\text{ m}$ . The calculated crack at serviceability limit state after being strengthened with prestressed steel wire ropes was 0.09 mm. The value of 0.09 mm was less than the value of 0.2 mm, which met the requirement.

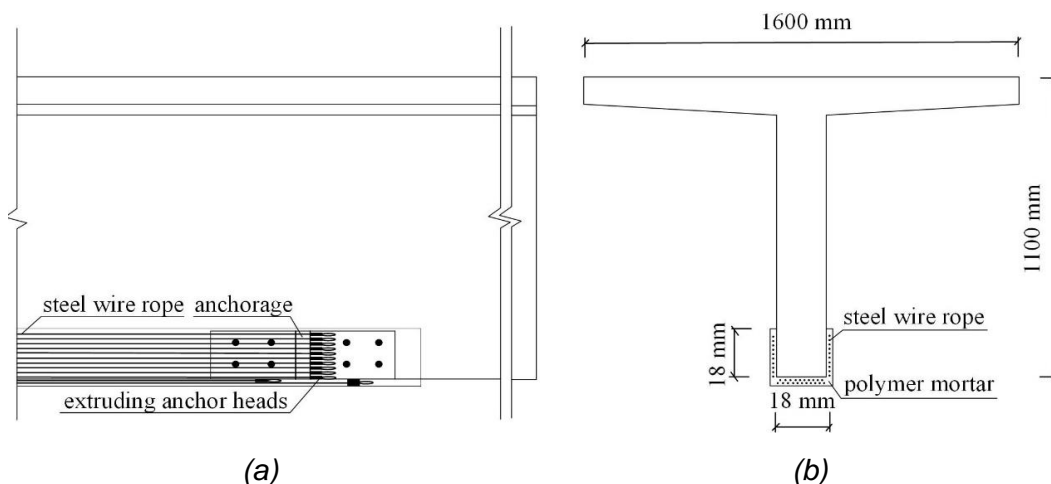


Fig. 7 - Diagram for the T-shape beam strengthened with steel wire ropes ;  
a) Lateral schematic diagram, b) Cross-section

## Strengthening process

Prestress steel wire ropes strengthening is similar to add prestressing by external tendons [18, 19], but the drawing space and dosage of scaffolding during construction for prestressed steel wire ropes is significantly less than adding prestressing by external tendons.

(a) Wire rope measuring (Figure 8(a)). Steel wire ropes were measured and cut into the same length according to the design.

(b) Extruding anchor heads making (Figure 8(b)). For the extruding anchor head, one end of a steel wire rope was folded into two, put through an aluminium alloy sleeve, and extruded to become an extruding anchor head through a squeezer, which could anchor a steel wire rope effectively. The applied anchorage was similar to a button-head anchorage – the length of the steel wire ropes was based on the designed tensile stress.

(c) Anchorage installing (Figure 8(d)). The U-shape steel plate was fixed on the beam end through high strength bolts and steel sticking glue. Weld anchorage was carried out on the steel plate. In order to ensure welding quality, the welding parts of steel plate were polished. Fig.8(d) shows the anchorage used in this bridge

(d) Tensioning and installing steel wire ropes (Figure 8(c) and Figure 8(d)). One end of a steel wire rope was put through an anchorage and the other was tensioned through a small tensioner. Tensioning is convenient in construction site owing to the flexibility of steel wire ropes. The steel wire rope was stretched and anchored when the extruding anchor head surpassed the anchorage. The value of tensioning force could be controlled by pre-design elongation value of the steel wire rope. A tension sensor was used to check the tensioning force in the construction site.

(e) Pouring mortar (Figure 8(e)). A U-shape wooden template was installed on the bottom of the T-beam. Polymer mortar was mixed through a blender and pressed into the template by grouting machine. To cope with the environment to which the steel wire ropes may be exposed, the polymer mortar could be used isolate steel wire ropes from natural conditions. Polymer mortar had satisfactory crack resistance and adhesion, relative to the ordinary mortar. The good liquidity and adhesion of polymer mortar could effectively wrap steel wire ropes. Thus, a relatively thin layer of polymer mortar increased the durability of the steel wire ropes.



(a) (b)

Fig. 8 - Main steps for strengthening; a) steel wire ropes tension, b) steel wire ropes installing

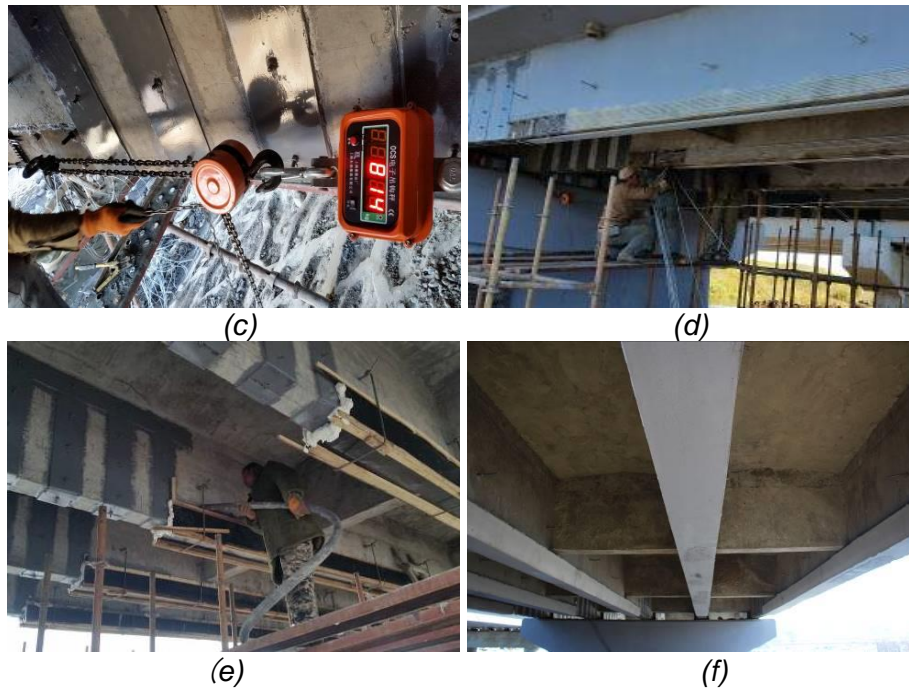


Fig. 8 - Main steps for strengthening; a) steel wire ropes tension, b) steel wire ropes installing, c) mortar pouring, d) steel wire ropes installing, e) mortar pouring, f) demolition of the template

## LOAD TEST

Before strengthening and two months after strengthening, load tests were performed to obtain the service ability of the bridge. These tests are repeated once a year and they will continue over a period of three years. Four three-axle trucks were used to apply simulated traffic loading to the structure. The gross rail loads of the test trucks before and after strengthening are listed in Table 2. The sequencing, in which the four trucks were designated A through D (Figure 9), consisted of Truck A, Trucks A+B, Trucks A+B+C, Trucks A+B+C+D, Trucks B+C+D, Trucks C+D, Trucks D. Due to the actual strength of the structure was not known, three truck positions were marked to gradually increase applied moment on the bridge. Truck locations in Figure 10 during the tests were determined to result in safe stress-levels.

Table 2. Gross axle load of trucks before and after strengthening

Load-test trucks		Force axle $t_1$ (kN)	Back axle $t_2$ (kN)	Back axle $t_2$ (kN)
Before	(A)	58.1	135.1	135.1
	(B)	58.0	134.2	134.2
	(C)	58.3	134.4	134.4
	(D)	59.4	136.9	136.9
After	(A)	59.0	135.2	135.2
	(B)	58.6	135.0	135.0
	(C)	59.1	136.4	136.4
	(D)	58.6	134.4	134.4

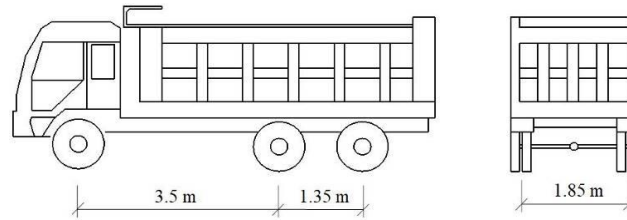


Fig. 9 - Load-test truck configuration

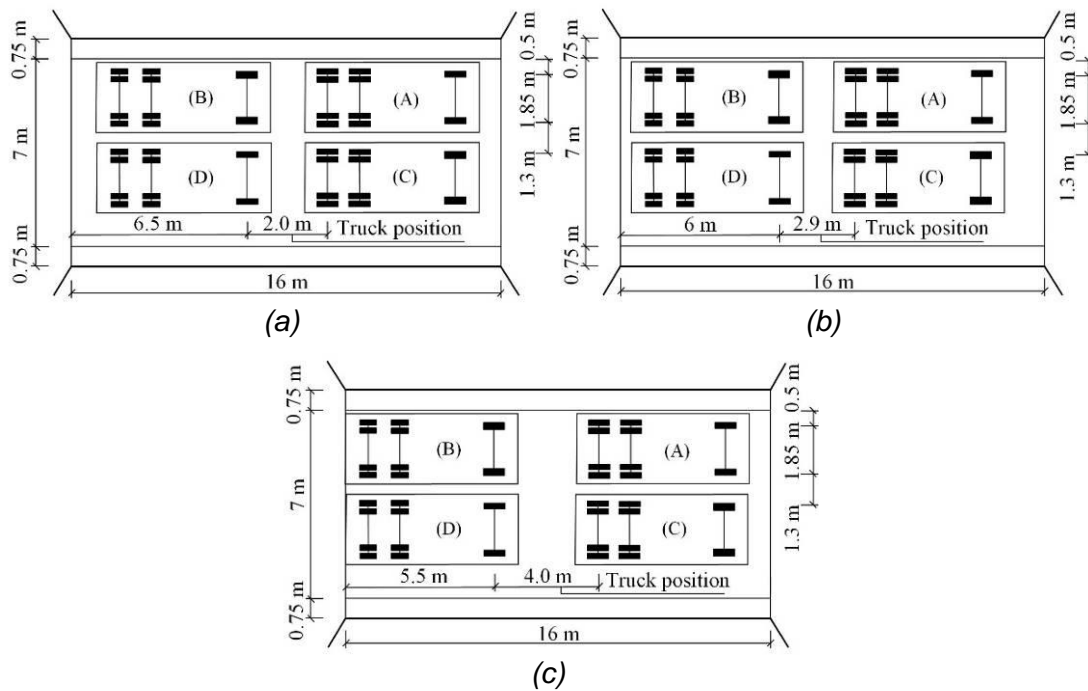


Fig. 10 - Distribution of load-test trucks on the bridge deck at different truck position; a) Truck position: 2.0 m, b) Truck position: 2.9 m, c) Truck position: 4.0 m

## STRAIN MEASUREMENT

All the recorded strain gauges were arranged at the midspan. The strain gauge arrangement of each beam was the same. In the “before” strengthening test, four strain gauges were installed on the concrete surface of each beam. In the “after” strengthening test, four gauges were placed on the concrete surface of each beam, which were the same as the “before” strengthening test. In addition, two gauges were placed on the surface of the steel wire ropes.

All the strain values were recorded at different loading stages, including no live load, Truck A, Trucks A+B, Trucks A+B+C, Trucks A+B+C+D, Trucks B+C+D, Trucks C+D, Trucks D and no live load, respectively.

The strain gauges were placed on the concrete surface at the mid-span in the “before” strengthening test and the “after” strengthening test, with the detailed locations shown in Figure 11(a). The letter *n* represents the beam number, and the letter C represents the concrete strain gauges. Resistance strain gauges (Cn1) were installed on the bottom of the beam before strengthening, as the bottom of the beams was covered with polymer mortar after strengthening. The strain gauges of the steel wire ropes are shown in Figure 11(b). The letter S represents the steel wire rope strain gauges. The gauge Sn1 was installed on the steel wire rope surface at the bottom of the beam.

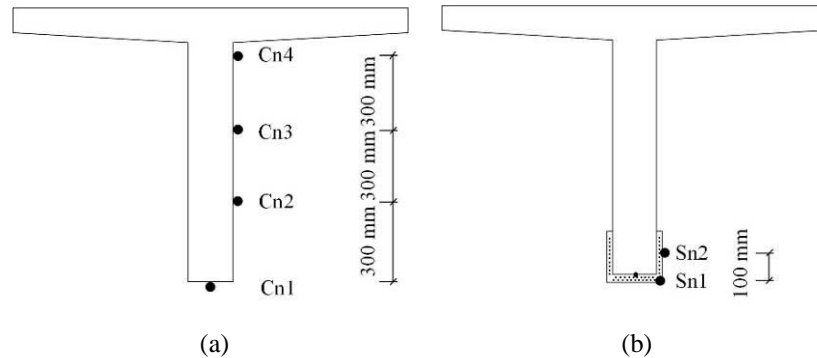


Fig. 11 - Locations of strain gauges mounted on the beams (*n* is the beam number); a) Strain gauges mounted on concrete; b) Strain gauges mounted on steel wire ropes

“Before” and “after” strengthening stains on concrete surface at midspans of beam 1-5, for the various truck combination at 4.0, 2.9 and 2.0-m positions on the bridge are shown in Figure 12. Comparing the “before” and “after” readings for gauges, it can be concluded that strengthening of the steel wire ropes obviously reduced concrete stress. The strain value was the largest when the sequencing was Trucks A+B+C+D. The maximum “before” strengthening strain of beam 1 was 225 microstrains for the case of all four trucks parked at 4.0-m position on the bridge because of the damage and the weak interaction between the beams. While, the maximum “after” strengthening strain of beam 1 was 200 microstrains. The strain was reduced to about 25 microstrains. The maximum “before” strengthening strain of beam 1 was 247 microstrains for the case of all four trucks parked at 2.9-m position. While, the maximum “after” strengthening strain of beam 1 was 219 microstrains. The strain was reduced to about 28 microstrains. The maximum “before” and “after” strengthening strains of beam 1 were 264 microstrains and 235 microstrains, respectively, for the case of all four trucks parked at 2.0-m position. Therefore, the concrete strain could be reduced after the prestressed steel wire ropes were used.

The recorded strain values of gauges Cn1, Sn1 and Sn2 of the five beams for the cases of all four trucks parked at different position are shown in Figure 13. In comparing the recorded concrete strains (gauge Cn1) and steel wire rope strains (gauge Sn1), the concrete strain values were approximately equal to the steel wire rope strain values on the same horizontal height, indicated that steel wire ropes were well anchored to the girders by anchorage and mortar and were acting as an effective part of the cross-section. Therefore, steel wire rope strain compatibility was well at the live load.

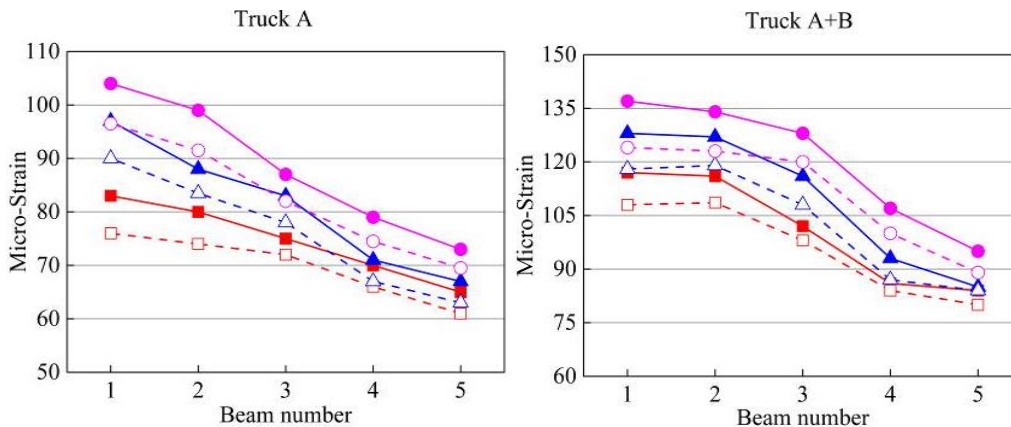


Fig. 12 - Maximum recorded strain ( $C_{n1}$ ) on concrete surface in the “before” and “after” strengthening

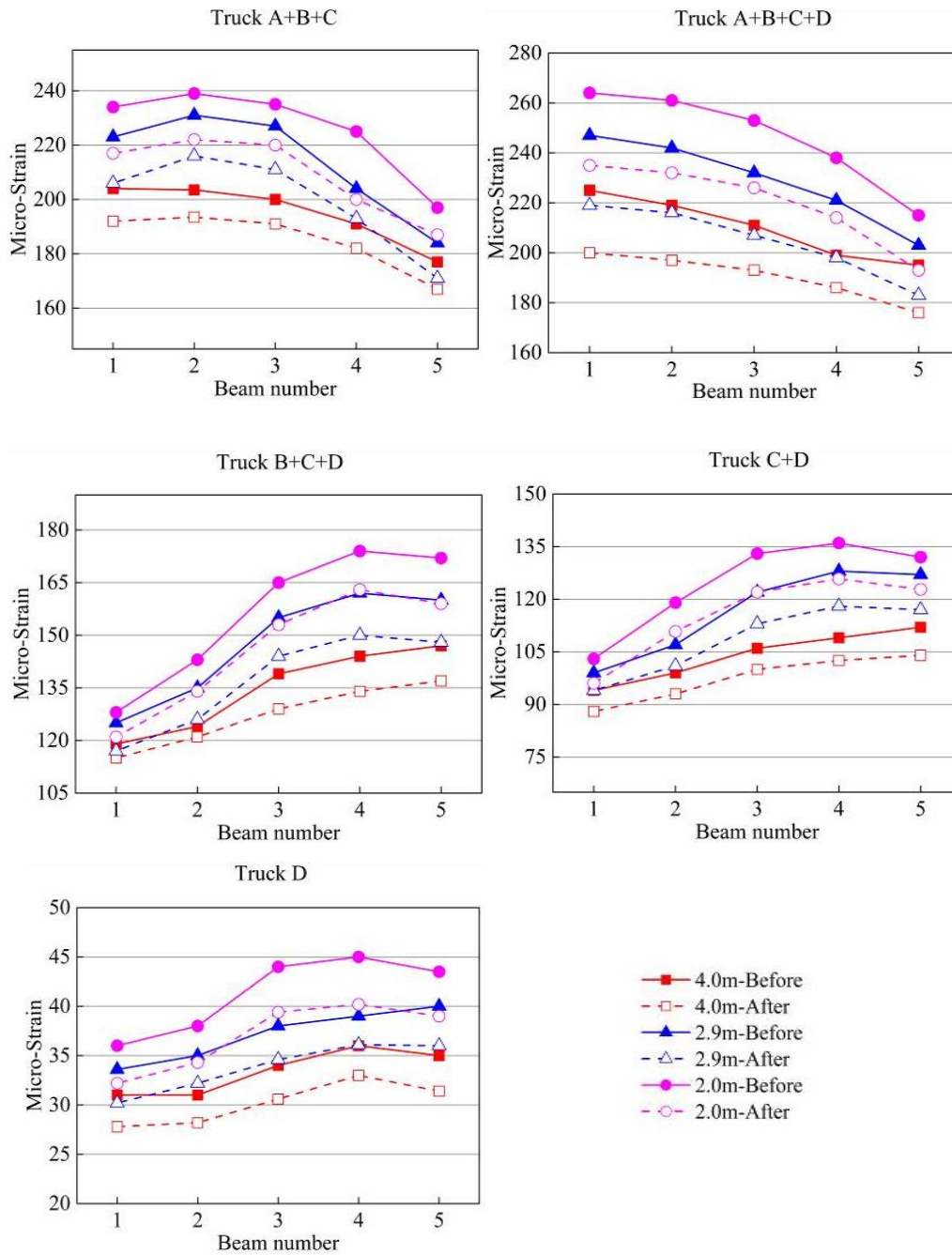
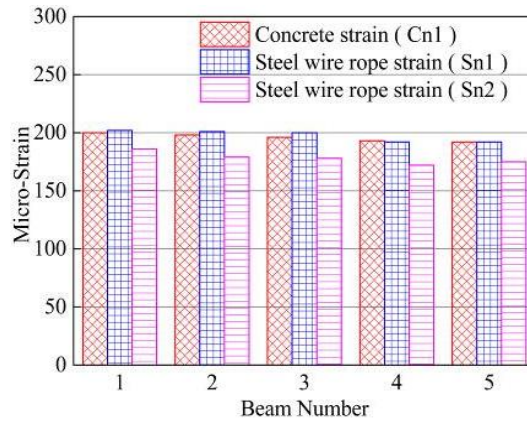
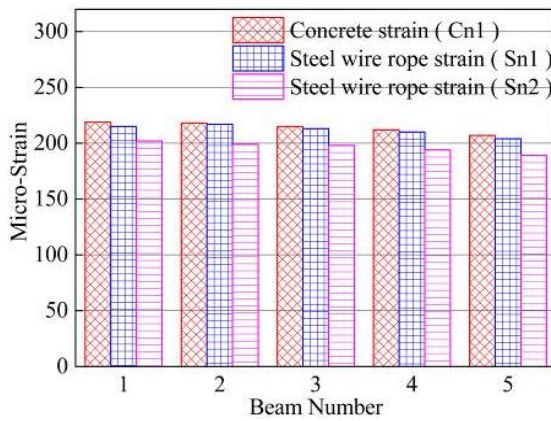


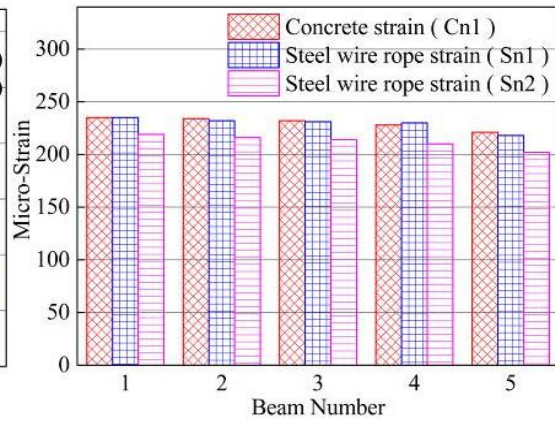
Fig. 12 - Maximum recorded strain ( $C_{n1}$ ) on concrete surface in the “before” and “after” strengthening



(a)



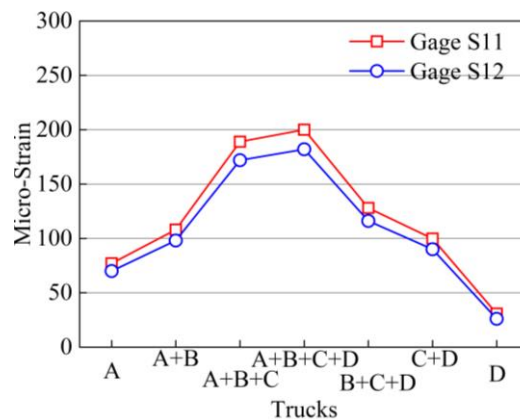
(b)



(c)

Fig. 13 - Concrete strains and steel wire rope strains for the case of all four trucks parked at different positions; a) 4.0-m position, b) 2.9-m position, c) 2.0-m position

Comparing the steel wire rope strains of gauge Sn2 with those recorded on gauge Sn1, the Sn2 strains were lower than the Sn1 strains. Strain compatibility led to the lower Sn2 strain than the Sn1 strain because steel wire rope at the bottom was physically located below steel wire rope at the side in the beam section.



(a)

Fig. 14 - Recorded strains for gauges mounted on steel wire ropes for cases of trucks parked at different positions

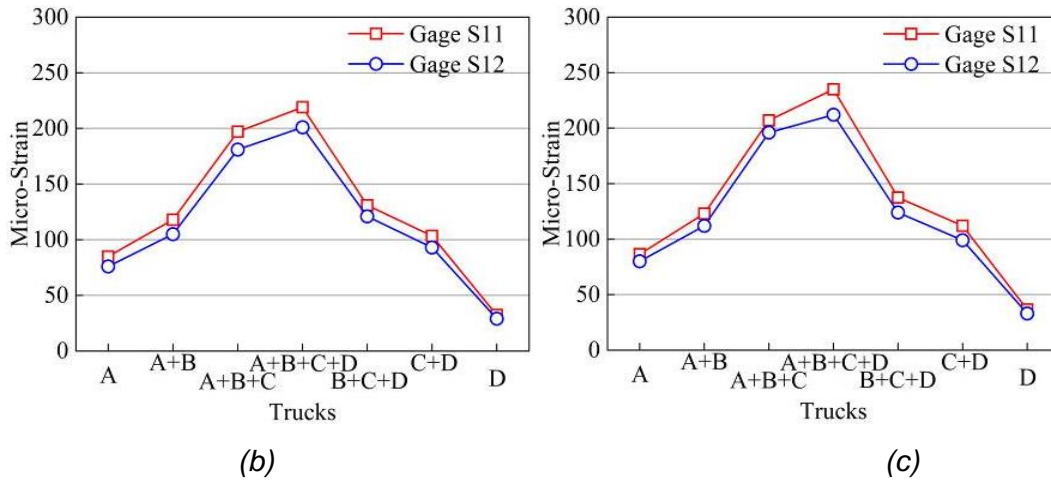


Fig. 14 - Recorded strains for gauges mounted on steel wire ropes for cases of trucks parked at different positions; a) 4.0-m position, b) 2.9-m position, c) 2.0-m position

Measured steel wire rope strains for the cases of trucks parked at different conditions and the various truck positions further confirmed consistency of the data and the effectiveness of the strengthening method in carrying load, as shown in Figure 14. From this figure, for the given truck position, reading from gauges S11 and S12 of beam 1 in 4.0-m, 2.9-m and 2.0-m position clearly showed that strains were proportional to applied bending.

The recorded strain values of beam 1 and beam 3 below the deck slab are listed in Table 3. The cases of four trucks parked at different conditions on the bridge. From this table, comparing the “before” and “after” strengthening strains for the given gauges, the compressive strains in the concrete were higher after the prestressed steel wire ropes were installed. In investigating this matter further, the neutral axes were determined as shown in Table 4. Four trucks (Trucks A+B+C+D) were parked on the bridge in 4.0-m condition. From this table, as expected, the neutral axis of beam 1 migrated downwards by about 20mm, after the steel wire ropes were installed in 4.0-m position. Meanwhile, the neutral axis of beam 1 migrated downwards by about 22mm and 24mm, when the cases of four trucks parked on the bridge in 2.9-m position and 2.0-m position, respectively.

Table 3 - Measured compressive strain on beam 1 and beam 3

Truck position (m)	Gauge C14 strain ( $\mu\epsilon$ )		Gauge C34 strain ( $\mu\epsilon$ )	
	Before	After	Before	After
4.0-m position	-7	-8	-6	-5
2.9-m position	-9	-11	-7	-6
2.0-m position	-10	-12	-9	-7

Table 4 - Neutral axis investigation

Truck position (m)	Before strengthening ( $\mu\epsilon$ )			After strengthening ( $\mu\epsilon$ )		
	Gauge C11 strain ( $\mu\epsilon$ )	Gauge C14 strain ( $\mu\epsilon$ )	Neutral axis location (mm)	Gauge C11 Strain ( $\mu\epsilon$ )	Gauge C14 strain ( $\mu\epsilon$ )	Neutral axis location (mm)
4.0-m position	225	-7	227	200	-11	247
2.9-m position	247	-9	232	219	-14	254
2.0-m position	264	-10	233	235	-16	257

## DEFLECTION MEASUREMENT

The recorded deflection gauges were arranged at the midspan and at the end of the beam, respectively. The deflection gauge arrangement of each beam was the same. In the “before” strengthening test, one deflection gauge was installed at the midspan, and two deflection gauges were installed at the end of each beam. In the “after” strengthening test, the deflection gauge arrangement was as the same as the “before” strengthening test.

All the deflection values were recorded at different loading stages, including no live load, Truck A, Trucks A+B, Trucks A+B+C, Trucks A+B+C+D, Trucks B+C+D, Trucks C+D, Trucks D and no live load, respectively.

“Before” and “after” strengthening deflection at midspans of beam 1-5, for the various truck combination at 4.0, 2.9 and 2.0-m positions on the bridge are shown in Figure 15. The maximum “before” strengthening deflection of beam 1 was 7.94mm for the case of all four trucks (Trucks A+B+C+D) parked at 4.0-m position on the bridge. While the maximum “after” strengthening deflection was 7.15mm when the prestressed steel wire ropes were installed. This showed a decrease of 9.9%, compared with “before” strengthening deflection. The “after” deflection of beam1 was 7.85mm, a 11.3% decrease over “before” strengthening deflection for all four trucks (Trucks A+B+C+D) parked at 4.0-m position. The maximum “before” deflections of beam 1 was 9.43mm. After strengthening, the “after” strengthening deflection was 8.55mm for four trucks (Trucks A+B+C+D) parked at 2.0-m position. This showed a decrease of 9.3%, compared with “before” strengthening deflection. As expected, a certain decrease in deflection after the application of prestressed steel wire rope reinforcement could be observed at different positions. These findings represent an initially good performance, although the long-term performance will be monitored throughout the next year.

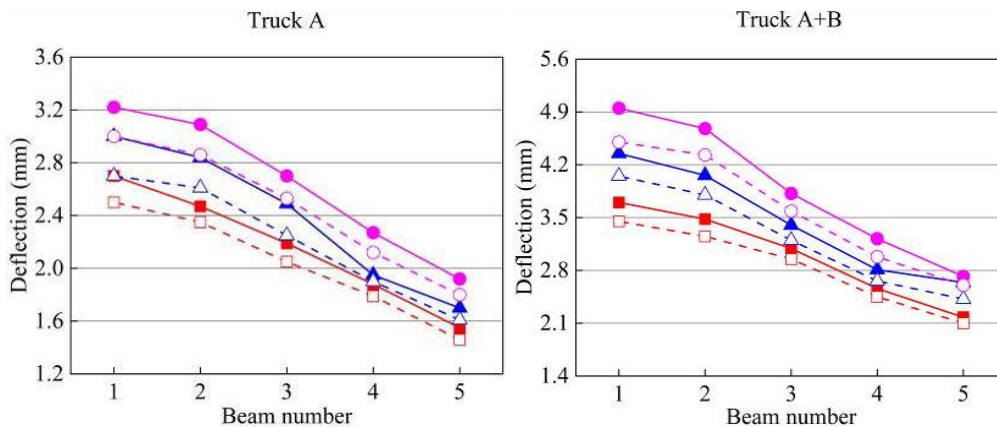


Fig. 15 - Maximum recorded deflection in the “before” and “after” strengthening

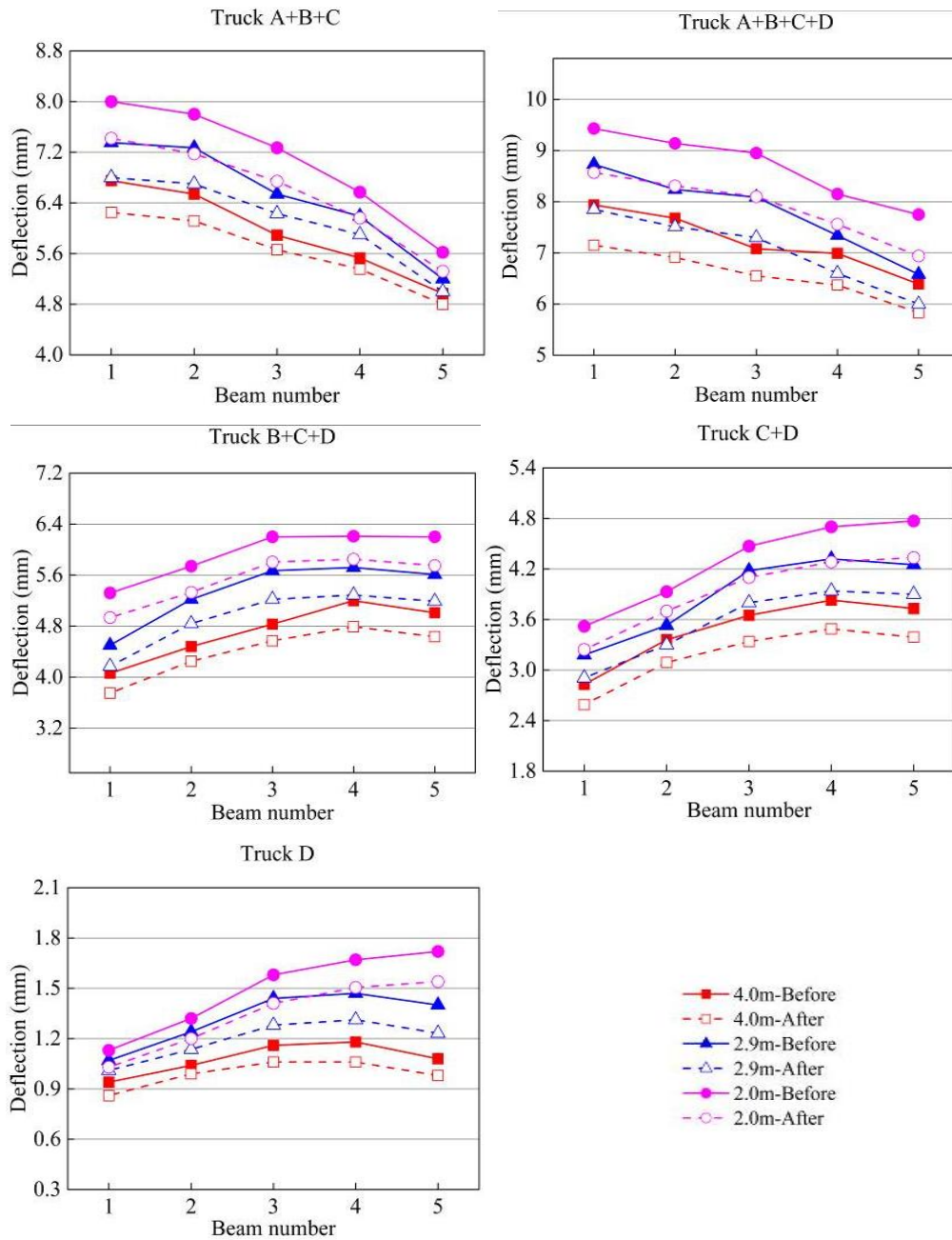


Fig. 15 - Maximum recorded deflection in the “before” and “after” strengthening

### CRACKS

The monitoring location of the crack in the “before” and “after” strengthening is shown in Figure 16. The width of the cracks increased with the test load increasing, but no new cracks appeared. These cracks had affected the durability of the bridge and would have further reduced the performance of the bridge if no actions were taken. In order to monitor the development of the cracks after strengthening, a repaired crack in the midspan of beam 1 was selected to be the monitoring crack of the load test. The crack width in the “before” and “after” strengthening is shown in Figure 17. The width of the crack on the soffit of the beam is 0.25mm for the case of all four

trucks (Trucks A+B+C+D) parked at 2.0-m position on the bridge before strengthening. The monitoring location of the crack is beyond the soffit of the beam, because concrete surface for the soffit of beams was covered with polymer mortar after strengthening. The depth from the monitoring location to the soffit of the beam was 20cm. The width of the crack at the monitoring location is 0.15mm before strengthening. Its width was unchanged for two trucks (Truck A+B), 0.03mm for three trucks (Trucks A+B+C), 0.05mm for four trucks (Trucks A+B+C+D) and closed when the trucks were moved from the deck. Furthermore, periodical inspections were carried out to observe the development of surface cracks on the side of the beams. The crack was found to be stable.

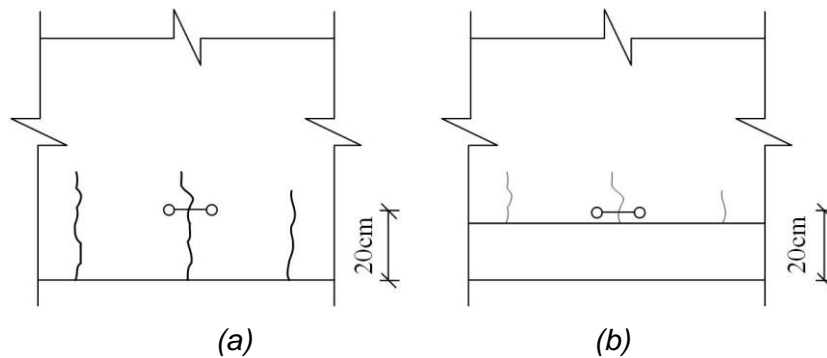


Fig. 16 - The monitoring location of the crack in the “before” and “after” strengthening;

a) “before” strengthening, b) “after” strengthening

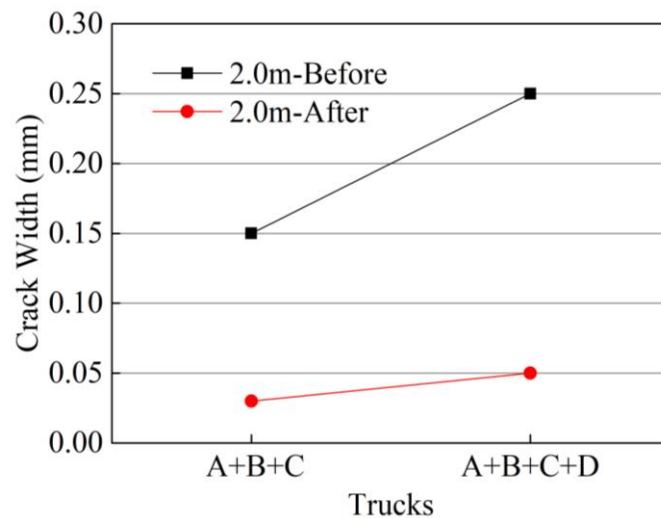


Fig. 17 - The crack width in the “before” and “after” strengthening

## LIVE-LOAD DISTRIBUTION FACTORS

The live load distribution factors (DFs) is by definition the fraction of the total load that anyone of the T-beam receives. The information on live-load DFs for a given bridge type and geometry can be obtained through field tests [20-22]. By measuring the deflection of every beam in the bridge under static loading, the DFs can be determined. As the geometric size of all the T-beams is almost the same, the stiffness of every beam can be considered as having an equal value. The  $DF_s$  can be determined from field measurements using the following.

$$DF_n = f_n / \sum f_n \tag{8}$$

Where  $f_n$  is the maximum static deflection in the nth girder, and  $n=1\sim5$ .

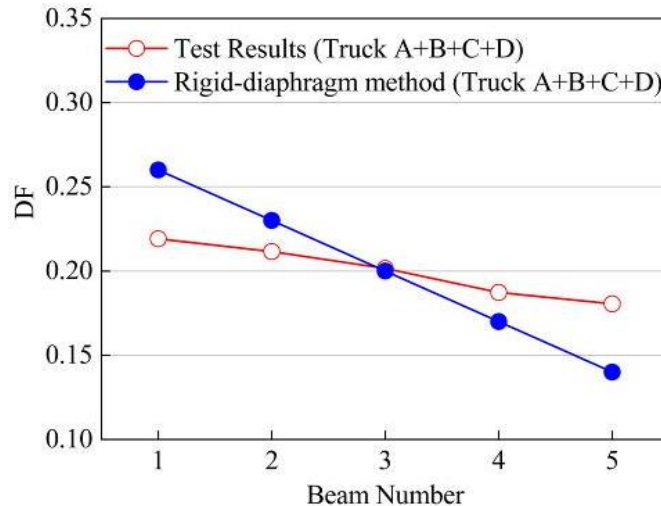


Fig. 18 - Live -load DFs calculated from test results and Rigid-diaphragm method for the case of all four trucks (Trucks A+B+C+D) parked at 2.0-m position

The deflection measurements shown in Figure 15 for the case of all four trucks (Trucks A+B+C+D) parked at 2.0-m position were used to determine the live-load DFs according to Equation. (8). From the rigid-diaphragm method [23], live-load DFs that can be compared with the measured DFs were provided as shown in Figure 18. The 1th girder (beam 1) deflected by 8.6mm for four trucks (Trucks A+B+C+D) parked at 2.0-m position. The total deflection of all the girders was 39.4mm for a live-load DF of about 8.6/39.4 or 0.22. The live-load DF is 0.26 using the rigid-diaphragm method. The live-load DFs depend on girder spacing, span, girder bending stiffness and girder torsional stiffness. The 2th girder (beam 2) deflected by 8.3mm for the four trucks (Truck A+B+C+D) parked at 2.0-m position. The total deflection of all the girders was 39.4mm for a live-load DF of about 8.3/39.4 or 0.21. The live-load DF is 0.23 using the rigid-diaphragm method. Thus, the rigid-diaphragm method is valid to evaluate the DFs of the T-shaped beam bridge after strengthening.

## CONCLUSION

An innovative strengthening technique was discussed to improve the flexural strength of a 20-year-old RC T-beam bridge with prestressed steel wire ropes in this paper. The detailed construction process was described. Load tests were conducted before and after installing the prestressed steel wire ropes to evaluate the effectiveness of the strengthening method. Based on the details presented in this paper and the results of the field-loading test, the following conclusions can be drawn:

The flexural strength of the RC T-beam bridge strengthened with steel wire ropes can be determined based on strain compatibility, force equilibrium, and the controlling modes of failure. The T-beam bridge strengthened with steel wire ropes is governed by the failure of concrete crushing.

The steel wire ropes strengthening increased the flexural capacity of the superstructure, and the deflection and crack width for girders were decreased in different degrees. Static load test

showed an initial good performance of the steel wire ropes strengthened spans. The long-term performance will be monitored throughout three years with annual load tests.

The steel wire rope strain deformation complies with strain coordination under the static load. Location of the neutral axis was observed to have migrated down after the steel wire ropes were installed.

The transverse connection between beams was proven by the diaphragm and the bridge deck. The live-load DFs of the strengthened bridge calculated by experimental results were in good agreement with the rigid-diaphragm method.

## REFERENCES

- [1] Jones R., Swamy R. N., Charif A., 1988. Plate separation and anchorage of reinforced concrete beams strengthened by epoxy-bonded steel plate. *Structural Engineer*, vol. 66, no. 5: 85-94
- [2] Sabahattin A., Ilker K., Bengi A., Sinan K., 2013. Strengthening and repair of reinforced concrete beams using external steel plates. *Journal of Structural Engineering*, vol. 139, no. 6: 929-939
- [3] Dae G. P., Byung H. O., Jae Y. C., 2003. Static and fatigue behavior of reinforced concrete beams strengthened with steel plates for flexure. *Journal of Structural Engineering*, vol. 129, no. 4: 527-535
- [4] Nabil F. G., Sayed G. A., Soliman A. K., Saleh K. R., 1999. Strengthening Reinforced Concrete Beams Using Fiber Reinforced Polymer (FRP) Laminates. *Aci Structural Journal*, vol. 188, no. 8: 865-875
- [5] Bakis C., 2002. Fiber Reinforced Polymer Composites for Construction—State-of-the-Art Review." *Journal of Composites for Construction*, vol.6, no. 2: 73-87
- [6] Mohammed A. S., Tarek M. K., Walid N.M., 2016. Analysis of RC Continuous Beams Strengthened with FRP Plates: A Finite Element Model. *Civil Engineering Journal*, vol. 2, no. 11: 576-589
- [7] Wojciech L., Ernest K., 2006. Behavior of composite beams prestressed with external tendons: Experimental study. *Journal of Constructional Steel Research*, vol. 62, no. 12: 1353-1366
- [8] Kiang H. T., Farooq M. A. A., Chee K. N., 2001. Behavior of simple-span reinforced concrete beams locally strengthened with external tendons. *Aci Structural Journal*, vol. 98, no. 2: 174-183
- [9] Keun-Hyeok Y., Dae-Bong J., Jae-Il S., Jae-Hoon K., 2012. In-plane seismic performance of unreinforced masonry walls strengthened with unbonded prestressed wire rope units. *Engineering Structures*, vol. 45: 449-459
- [10] Liao Z., Zhang C., Jia T., Wang H., 2017. Experimental investigation on seismic behavior of shear wall retrofitted with pre-stressed steel wire mesh and polymer mortar. *Journal of Building Structures*, vol. 38, no. 6: 70-77
- [11] Guo J., Deng Z., Lin J., Lu H., 2014. Experimental study on seismic behaviour of RC columns strengthened with prestressed high strength steel wire mesh. *Journal of Building Structures*, vol. 35, no. 2: 128-136.
- [12] Guo J., Deng Z., Lin J., Lu H., 2014. Experimental study on seismic behaviour of RC columns strengthened with prestressed high strength steel wire mesh. *Journal of Jilin University*, vol. 44, no. 4
- [13] Gang W., Zhishen W., Yang W., Jianbiao J., and Yi C., 2012. Flexural strengthening of RC beams using distributed prestressed high strength steel wire rope: theoretical analysis. *Structural and Infrastructure Engineering*, vol. 10, no. 2: 160-171
- [14] Gang W., Jianbiao J., Wu Z. S., Zhang M., 2010. Experimental study of RC beams strengthened with distributed prestressed high-strength steel wire rope. *Magazine of concrete research*, vol. 62, no. 4: 253-265
- [15] Zhang Y., Xu S., Yao X., 2010. Theoretical Analysis and Experiment on Flexural Strengthening Behaviors of Prestressed High-strength Steel Wire ropes and Polymer Mortar. *China Journal of Highway and Transport*, vol. 30, no. 6: 239-248
- [16] Ministry of Communications of China, 1985. Design Code of Highway Reinforced Concrete and Prestressed Concrete Bridge (JTJ023-85). China Communication Press: Beijing.

- [17] Ministry of Communications of China, 2010. Design Code of Concrete Structures (GB50010). China Building Industry Press: Beijing.
- [18] Yail J. K., Mark G., Garth J. F., 2008. Repair of Bridge Girder Damaged by Impact Loads with Prestressed CFRP Sheets. Journal of Bridge Engineering, vol. 13, no. 1: 15-23
- [19] Hamdy M. E. A., Ahmed M. A., Salah E. F. T., 2012. Behavior of Strengthened Composite Castellated Beams Pre-stressed with External Bars: Experimental Study. Arabian Journal for Science and Engineering, vol. 37, no. 6 : 1521-1534
- [20] Junsik E., Andrzej S. N., 2001. Live Load Distribution for Steel Girder Bridges. Journal of bridge Engineering, vol. 6, no. 6: 489-497
- [21] Janusz, Holowaty, 2013. Assessment of Numerical Models for Live Load Distribution in a Road Slab Bridge. Computer Technology and Application, vol. 4,: 591-598
- [22] Michael S., Jeffrey A. L., 2001. Response of Prestressed Concrete I-Girder Bridges to Live Load. Journal of bridge engineering, vol. 6, no.1: 1-8
- [23] Ministry of Communications of China, 2015. General Specification for Highway Bridge and Culvert Design (JTG D60). China Communication Press: Beijing.